HANDLING ELECTROSTATIC INTERACTIONS IN MOLECULAR SIMULATIONS: A SYSTEMATIC STUDY

Jiří KOLAFA[a], Filip MOUČKA[b] and Ivo NEZBEDA[b,c,*]

[a] *Department of Physical Chemistry, Institute of Chemical Technology, Prague, 166 28 Prague 6, Czech Republic; e-mail: jiri.kolafa@vscht.cz*

[b] *Faculty of Science, J. E. Purkinje University, 400 96 Ústí nad Labem, Czech Republic; e-mail: moucka@seznam.cz*

[c] *E. Hála Laboratory of Thermodynamics, Institute of Chemical Process Fundamentals, Academy of Sciences of the Czech Republic, 165 02 Prague 6, Czech Republic; e-mail: ivonez@icpf.cas.cz*

Received December 10, 2007
Accepted March 10, 2008
Published online April 25, 2008

Dedicated to Professor William R. Smith on the occasion of his 65th birthday.

Two qualitatively different models with strong long-range electrostatic interactions, Lennard–Jones diatomics with an embedded dipole moment and TIP4P/2005 water, are considered in extensive Monte Carlo and molecular dynamics simulations to systematically study the differences in results caused by different treatments of the long-range electrostatic interactions. In addition to the standard Ewald summation and reaction field methods, we consider also two variants of short-range approximations. Both thermodynamic and structural properties, and both homogeneous and inhomogeneous phases are considered. It is shown that the accuracy of the short-range approximations with carefully selected parameters may be sufficient for a number of applications; however, in some cases one can encounter accuracy limits or structural or other artifacts.

Keywords: Molecular simulation; Ewald summation; Reaction field; Long-range interactions; Electrostatic forces.

With the fast development of computer technology and the associated availability of fast and powerful computers, molecular simulations[1] have become a routine 'experimental' tool to study various processes and properties of matter on molecular level. Both commercial (e.g., ref.[2]) and freeware (e.g., refs[3,4]) software packages are available and all these facts may build the impression that all (basic) methodological and technical problems of molecular simulations have been successfully solved and that carrying out simulations is really a safe and routine approach free of potential pitfalls.

Collect. Czech. Chem. Commun. 2008, Vol. 73, No. 4, pp. 481–506

doi:10.1135/cccc20080481

However, this is by no means true. Intermolecular interaction models of non-simple compounds include unavoidably long-range electrostatic interactions whose strength does not become negligibly small at large distances and the question how to treat them correctly (and efficiently) does not seem to have been satisfactorily answered yet, which becomes evident from again and again appearing papers with contradicting conclusions.

There have been a number of methods commonly used to treat the long-range interactions: (i) simple spherical cutoff, (ii) the Ewald summation, (iii) reaction field method (RF) for dipolar systems, and (iv) multipole expansion, and their various modifications. Each method has its own advantages and disadvantages. In addition to their accuracy, the choice of the method is often dictated also by its simplicity and efficiency.

The Ewald summation[1,5] has become a standard tool to handle long-range electrostatic interactions. Nonetheless, in addition to its computational cost it has been questioned regarding possible artifacts caused by the imposed periodicity in the summation. The reaction field method[6,7] should yield the same results as the Ewald sum but becomes inapplicable to systems with charged objects. Moreover, the application of both these methods, i.e., the Ewald sum and reaction field, is somewhat problematical when they are to deal with inhomogeneous systems. Very likely for these reasons the simplest approach, the spherical cutoff, which neglects all interactions beyond a certain distance, has been frequently used[8]. Its use is based on the conviction that a sufficiently large cutoff may make the neglected interactions negligibly small. However, as it has been demonstrated in numerous papers, this is not true. For instance, applying the simple cutoff method to the original TIP5P potential of water[9] we showed[10] that the energy does not bear any sign of convergence with a gradual increase of the cutoff distance and that the potential model in fact does not reproduce the properties it was adjusted to. This finding prompted then Rick[11] to reparametrize the TIP5P model accounting carefully for the long-range corrections. Although some properties may be rather insensitive to the long-range corrections, others may be severely affected. Even more, the use of the cutoff method may give rise to strange artifacts as it has been shown recently by Yonetani[12,13] and confirmed later by van der Spoel and van Maaren[14]. Although the use of the cutoff method may still be reported it is more than evident that it should be taken out from the list of potential simulation methods when one deals with systems that include long-range interactions.

An alternative method to treat long-range forces, particularly gravity and, to some extent, also the Coulombic forces, is the fast multipole expansion,

also known as the Greengaard–Rokhlin method or tree code[15]. In the case of the Coulombic forces it converges much more slowly than for gravity and becomes thus advantageous only for very large systems[16]; therefore, it will not be considered here.

The project, whose results are presented in this paper, has been motivated primarily by a recent paper by Fennell and Gezelter[17] entitled 'Is the Ewald summation still necessary?'. In this paper the authors summarize and optimize short-range electrostatic methods inspired by the Ewald *r*-space form (the true electrostatic potential is damped using the erfc function, further shifted and truncated into a short-range potential). They conclude that '... results do suggest that in the typical simulations performed today, the Ewald summation may no longer be required ...'.

In our opinion the above conclusion may be correct only for certain properties and under certain circumstances and, although the list of types of considered system may seem impressive, our experience tells us that it cannot be expected in general. For instance, vapor–liquid equilibria, the property of high importance for the chemical engineering community, have not been included into the list of examined properties. Similarly, purely dipolar (non-associating) fluids that seem to be more sensitive to the treatment of the long-range interactions than associating fluids have not been considered at all. In addition, there are several forms of the short-range electrostatics which differ in implementation details, smoothness, efficiency, etc.

The purpose of this paper therefore is to carefully reexamine, along with another available approximation[4], the short-range approximation of Fennell and Gezelter and to find properties for which, and conditions at which, they can be safely used and save computing efforts or, alternatively, when their application may lead to inaccurate or even erroneous/misleading results. We consider the shifted force variant of the short-range approximation and compare its results with those obtained using the standard Ewald summation (or its 2D variant corrected for the slab dipole moment[18] in the case of inhomogeneous fluids), the reaction field method, and the short-range electrostatics version as built for years into the MACSIMUS package[4]. In addition to water modeled by the recently developed TIP4P/2005 potential[19] (likely the most accurate nonpolarizable model of water available to date), we consider also a dipolar fluid modeled by the Lennard–Jones diatomic potential with embedded dipole. The properties considered include the equilibrium, both thermodynamic and structural, properties of homogeneous systems, and the thermodynamic and interfacial properties of the liquid and vapor phases at equilibrium.

BASIC DEFINITIONS AND COMPUTATIONAL DETAILS

Models

In the present paper we consider two qualitatively different models of strongly polar fluids: (i) non-associating fluid modeled by dipolar Lennard–Jones diatomic molecules (DLJD), and (ii) water (W), modeled by the TIP4P/2005 potential[19]. Explicit forms of the respective intermolecular potentials read, in general, as follows:

$$u_{\mathrm{DLJD}}(1,2) = \sum_{i,j} u_{\mathrm{LJ}}(r_{ij}) + u_{\mathrm{DD}}(\boldsymbol{R}_{12}) \tag{1}$$

and

$$u_{\mathrm{W}}(1,2) = u_{\mathrm{LJ}}(R_{12}) + u_{\mathrm{Coul}}(1,2) \tag{2}$$

where r_{ij} denotes the intermolecular separation between site i on molecule 1 and site j on molecule 2, $R_{12} = |\boldsymbol{R}_{12}|$ is the intermolecular center-to-center separation, and

$$u_{\mathrm{LJ}}(r) = 4\varepsilon\left[\left(\frac{\sigma}{r}\right)^{12} - \left(\frac{\sigma}{r}\right)^{6}\right] \tag{3}$$

$$u_{\mathrm{Coul}}(1,2) = \sum_{i,j} \frac{q_i q_j}{r_{ij}} \tag{4}$$

where q_i are partial charges in the CGS units.

As for the u_{DD} term, to make the LJ diatomic molecule polar, one may either embed into it a point dipole or to use appropriately distributed charges. For technical reasons we use the latter approach with two charges placed symmetrically on the axis of the diatomics but, to make a close contact with the paper by Mecke et al.[20] who considered a point dipole, we place the charges only infinitesimally apart making the electric field essentially identical to the point dipole. Thus,

$$u_{\mathrm{DD}} = \frac{\mu^2}{R_{12}^3}\left[\boldsymbol{\nu}_1\boldsymbol{\nu}_2 - 3\frac{(\boldsymbol{\nu}_1\cdot\boldsymbol{R}_{12})(\boldsymbol{\nu}_2\cdot\boldsymbol{R}_{12})}{\boldsymbol{R}_{12}}\right] \approx \sum_{i,j}\frac{q_i q_j}{r_{ij}} \tag{5}$$

where $\boldsymbol{\mu} = \mu\boldsymbol{\nu}$ is the dipole moment in the direction of the axis of the molecule $\boldsymbol{\nu}$ ($|\boldsymbol{\nu}| = 1$) and $\mu = |q_i|l$. We set $l/\sigma = 3 \times 10^{-4}$ in all computations; the expected systematic error compared with the point dipole is of the order of $(l/\sigma)^2 \approx 10^{-7}$. Furthermore, we use the usual reduced units, i.e., $T^* = k_B T/\varepsilon$, $\mu^* = \mu/\sqrt{\varepsilon\sigma^3}$, and $L^* = L/\sigma$, where k_B is the Boltzmann constant and L is the site–site span of the diatomic molecule.

For details on the TIP4P/2005 potential, we refer the reader to the original paper[19].

Electrostatic Forces

Long-Range Approaches

When forces acting between the molecules are long-ranged, and one still wants to keep the cubic periodic boundary conditions as the approximation leading to the most accurate results for a given finite number of molecules N, the following infinite sum over periodic images has to be evaluated:

$$U_{\mathrm{Coul}} = \frac{1}{2}\sum_{\boldsymbol{n}}{}' \left(\sum_{i}^{N}\sum_{j}^{N} \boldsymbol{u}_{\mathrm{Coul}}(|\boldsymbol{r}_{ij} + \boldsymbol{n}|) \right). \tag{6}$$

The sum is over all integer vectors $\boldsymbol{n}$ and the prime means that terms $i = j$ are omitted for $\boldsymbol{n} = 0$. The summation in Eq. (*6*) is only conditionally convergent but may be transformed into two absolutely and rapidly convergent series, one in the real space and the other in the reciprocal k-space,

$$U = \sum_{\boldsymbol{n}}{}' \sum_{1 \le j \le l \le N} \frac{q_j q_l \,\mathrm{erfc}(\alpha|\boldsymbol{r}_j - \boldsymbol{r}_l + \boldsymbol{n}L|)}{|\boldsymbol{r}_j - \boldsymbol{r}_l + \boldsymbol{n}L|}$$

$$+ \sum_{\boldsymbol{k},\boldsymbol{k}\neq 0} \frac{\exp(-\pi^2 k^2/\alpha^2 L^2)}{2L\pi k^2} |Q(\boldsymbol{k})|^2 + \frac{2\pi}{2\varepsilon' + 1}\frac{\boldsymbol{M}^2}{L^3} - \frac{\alpha}{\sqrt{\pi}}\sum_{j=1}^{N} q_j^2 \tag{7}$$

where

$$Q(\boldsymbol{k}) = \sum_{j=1}^{N} q_j \exp(2\pi \mathrm{i}\boldsymbol{k}\cdot\boldsymbol{r}_j/L) \tag{8}$$

is the Fourier transform of the charge distribution, $\boldsymbol{M}$ is the total dipole moment of the simulation cell, and ε' is the dielectric constant of a continuum surrounding the simulation cell at infinity (for the precise definition, see

ref.[21]). Parameter α, sometimes called separation or damping parameter, influences the efficiency of the summation. Note also that we use the CGS system of units; in the SI units, the electrostatic energy is multiplied by $1/(4\pi\varepsilon_0)$, where ε_0 is the permittivity of vacuum and ε′ becomes the relative permittivity.

In addition to the Ewald method, we consider also the reaction field method[7]. In this method the dipolar molecular system beyond the cutoff radius is replaced by a dielectric continuum. For the site–site potentials, the long-range corrections are then conveniently incorporated directly into the pair potential energy[22],

$$u_{\mathrm{Coul}} = \sum_{i\in\{1\}}\sum_{j\in\{2\}} \frac{q_i q_j}{r_{ij}} \left[1 + \frac{\varepsilon' - 1}{2\varepsilon' + 1} \left(\frac{r_{ij}}{R_c} \right)^3 \right]. \qquad (9)$$

We used the metal-like conditions, ε′ = ∞, both in the Ewald summation, Eq. (*7*), and in the reaction field for DLJD. For water calculations we used ε′ = 80 in the Ewald method while ε′ = ∞ in the reaction field.

Short-Range Approximations

The computational costs of the Ewald summation and other methods taking into account the long-range nature of the electrostatic interactions may be bypassed by making the electrostatic interactions effectively short-ranged, which makes it then possible to confine all considerations to a range within the cutoff radius, R_c. Fennell and Gezelter[17] consider two variants of such an approach, the damped shifted potential (SP) version and damped shifted force (SF) version. In these versions the Coulomb interaction is approximated as follows (for details, see the original paper[17]):

$$u_{\mathrm{SP-FG}} = q_i q_j \left[\frac{\mathrm{erfc}(\alpha r)}{r} - \frac{\mathrm{erfc}(\alpha R_c)}{R_c} \right], \quad \text{for } r \le R_c \qquad (10)$$

and

$$u_{\mathrm{SF-FG}} = q_i q_j \left\{ \frac{\mathrm{erfc}(\alpha r)}{r} - \frac{\mathrm{erfc}(\alpha R_c)}{R_c} + \left[\frac{\mathrm{erfc}(\alpha R_c)}{R_c^2} + \frac{2\alpha \exp(-\alpha^2 R_c^2)}{R_c \sqrt{\pi}} \right] (r - R_c) \right\}, \quad \text{for } r \le R_c \qquad (11)$$

and in both cases the potential is zero for $r \geq R_c$. The forces associated with these potentials read

$$F_{\mathrm{SP-FG}} = q_i q_j \left[\frac{\mathrm{erfc}(\alpha r)}{r^2} + \frac{2\alpha \exp(-\alpha^2 r^2)}{r\sqrt{\pi}} \right], \quad \text{for } r \leq R_c \tag{12}$$

and

$$F_{\mathrm{SP-FG}} = q_i q_j \left\{ \left[\frac{\mathrm{erfc}(\alpha r)}{r^2} + \frac{2\alpha \exp(-\alpha^2 r^2)}{r\sqrt{\pi}} \right] - \left[\frac{\mathrm{erfc}(\alpha R_c)}{R_c^2} + \frac{2\alpha \exp(-\alpha^2 R_c^2)}{R_c \sqrt{\pi}} \right] \right\}, \quad \text{for } r \leq R_c \tag{13}$$

respectively. The force of the SP-FG method suffers from discontinuity at the cutoff distance. In the SF-FG version the forces are continuous at the cutoff distance and only this version, suitable for most molecular dynamics (MD) simulations, is therefore considered henceforth.

In the MACSIMUS (M) package[4], the following form of short-range electrostatic forces is adopted,

$$u_{\mathrm{M}} = q_i q_j \times \begin{cases} 1/r - \Delta & \text{for } r < cR_c \\ (r - R_c)^3 (A + Br) & \text{for } cR_c < r < R_c \\ 0 & \text{for } r < R_c \end{cases} \tag{14}$$

where c is a dimensionless parameter (denoted as α in MACSIMUS). Parameters A, B, and the potential shift Δ are uniquely determined from the requirement that, at $r = cR_c$, the potential and its first and second derivatives be continuous. From the $(r - R_c)^3$ term in the potential it follows that the same continuity condition applies also at $r = R_c$. The SF-FG potential is not so smooth because its second derivative is not continuous.

The exact $(1/r)$ and approximate electrostatic potentials for unit charges are drawn in Fig. 1 and the forces $(1/r^2)$ in Fig. 2. All the short-range potentials are shifted and smoothed so that they are zero beyond the cutoff. More details can be seen from the forces in Fig. 2. Here the SF-FG forces are smaller than the exact term $1/r^2$ because they are also shifted, but then they behave more uniformly. The SP-M forces are not shifted at short separations. Consequently, they decay to zero less uniformly for larger c.

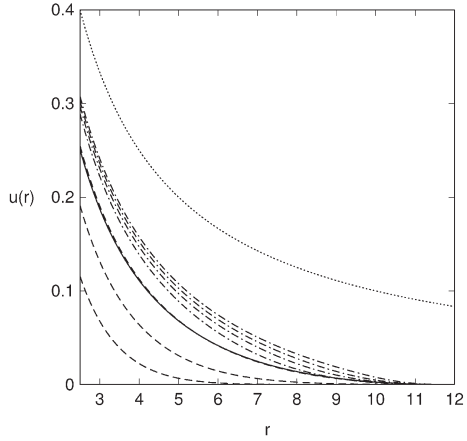

FIG. 1
The exact (dotted line), approximated dimensionless electrostatic energy $u(r) = 1/r$. Solid line: SF-FG, $\alpha = 0$. Dashed lines (from top): SF-FG, $\alpha = 0.1, 0.2, 0.3$. Dash-and-dotted lines (from top): SP-M $\alpha = 0.8, 0.7, 0.6, 0.5$

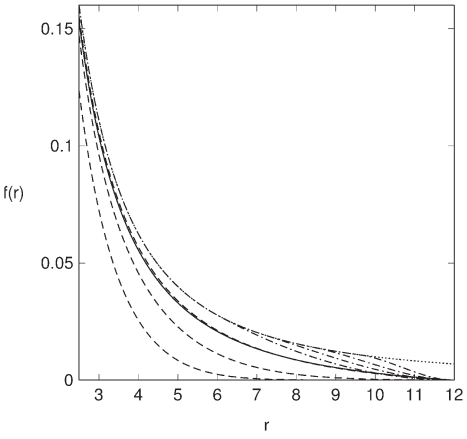

FIG. 2
The exact, approximated dimensionless electrostatic force $f(r) = 1/r^2$. The meaning of the lines is the same as in Fig. 1

Measured Quantities

The list of properties we evaluate in simulations and use in the discussion include:

1. For homogeneous systems, in addition to the standard thermodynamic functions, pressure (P) and residual internal energy (U), we consider also all site–site correlation functions g_{ij}, and the dipole–dipole correlation functions G_l of the 1st and 2nd order (called also 'local g-factors'[23]), dielectric constant (relative permittivity) ε, and diffusivity D. We use the MD simulations implemented with the Ewald summation and both short-range approximations (SF-FG and SP-M). Simultaneously, we use also the Monte Carlo (MC) method with the reaction field.

2. For inhomogeneous systems we determine the vapor–liquid equilibrium (VLE) properties using both the Gibbs ensemble MC (GEMC) simulations implemented with the reaction field method, and MD simulations with the explicit interface implemented with the 2D Ewald summation and short-range methods, the latter allowing to determine also the surface tension and various profiles in dependence on the distance from the surface.

Pressure is given by a general formula

$$P = \frac{N}{V} k_{\mathrm{B}} T - \frac{1}{3V} \left\langle \frac{\partial U}{\partial V} \right\rangle . \qquad (15)$$

This formula can be implemented in several ways. The most fool-proof method, called the virtual volume change (VVC) method[24], evaluates the partial derivative in Eq. (*15*) numerically,

$$P_{\mathrm{VVC}} = \frac{N}{V} k_{\mathrm{B}} T - \frac{1}{3V} \frac{U(V + \Delta V) - (U - \Delta V)}{2\Delta V} \qquad (16)$$

where $U(V \pm \Delta V)$ is implemented in periodic boundary conditions by scaling the positions of molecules (reference points) in the whole box. For pairwise forces, Eq. (*15*) can be rewritten to the virial of force (VoF) form,

$$P_{\mathrm{VoF}} = \frac{N}{V} k_{\mathrm{B}} T - \frac{1}{3V} \left\langle \sum_{i<j} r_{ij} u'_{ij}(r_{ij}) \right\rangle . \qquad (17)$$

For electrostatic forces, $u_{ij} = q_i q_j / r_{ij}$. The VoF (the sum above) equals the electrostatic energy which is readily available both in MC and MD simulations. We denote this pressure as $P_{V=E}$.

For rigorous electrostatic methods (Ewald summation, reaction field), Eq. (*18*) exactly holds

$$P_{VoF} = P_{V=E} \tag{18}$$

and the virial of electrostatic force does not have to be separately calculated (in fact, it would be probably very cumbersome to perform it for the *k*-space part of the Ewald sums). However, this equality is no longer valid for various short-range approximations! Consequently, we get two different approximations for pressure and it is not a priori known which is better. On the other hand, the relation

$$P_{VoF} \approx P_{VVC} \tag{19}$$

holds only approximately because of statistical and numerical errors.

The surface tension was evaluated from the pressure using the relation

$$\gamma = -\frac{3L_z}{4} P \tag{20}$$

where L_z is the box size in the *z*-direction (perpendicular to the slab) and *P* is the pressure calculated for the whole box by any of the above methods. This formula differs from the true result by a term proportional to $\langle z_i \, \mathrm{d}U/\mathrm{d}z_i \rangle$. However, this term is proportional to the vapor tension which is negligible in our case.

The diffusivity is computed from the linear term of linear regression of the squared displacement (SD)

$$\mathrm{SD}(t) = \frac{1}{6N} \sum_i [\boldsymbol{r}_i(t) - \boldsymbol{r}_i(0)]^2 . \tag{21}$$

The initial portion of the above squared displacement is omitted and the calculation is repeated over (overlapping) blocks (see ref.[25] for details).

The site–site and dipole–dipole correlation functions are defined, respectively, as follows:

$$4\pi r_{ij}^2 g_{ij}(r_{ij}) = \left(1 - \frac{1}{N}\right) V \left\langle \delta(r_{ij} - |\boldsymbol{r}_{1,i} - \boldsymbol{r}_{2,j}|) \right\rangle \tag{22}$$

and

$$4\pi r^2 G_l(r) = \left(1 - \frac{1}{N}\right) V \left\langle \delta(r - |\boldsymbol{r}_{1,\mathrm{O}} - \boldsymbol{r}_{2,\mathrm{O}}|) P_l(\cos\Theta_{12}) \right\rangle \tag{23}$$

where N is the number of molecules, V is the volume, P_l is the normalized Legendre polynomial, $\boldsymbol{r}_{1,i}$ denotes the position of site i on molecule 1, Θ_{12} is the angle formed by the axes of molecules 1 and 2, δ is the Dirac delta distribution, and $\langle\cdot\rangle$ denotes an ensemble average.

The dielectric constant ε was evaluated from the fluctuation formula[21] (cf. also equivalent approach[7,26])

$$\frac{(\varepsilon - 1)(2\varepsilon' + 1)}{2\varepsilon' + \varepsilon} = \frac{4\pi \left\langle \boldsymbol{M}^2 \right\rangle}{3k_{\mathrm{B}} TV} . \tag{24}$$

In the simulations with the Ewald summation, Eq. (*7*), we used for the surrounding dielectric continuum a rounded experimental value, $\varepsilon' = 80$. Since there is no interaction of the simulation cell dipole moment with the surrounding continuum (second last term in Eq. (*7*) in the short-range approximations, $\varepsilon' = \infty$ (tin-foil boundary conditions) should be used in Eq. (*24*).

Simulation Setup

For studying homogeneous phases by MC simulations we used the conventional simulations in an NVT ensemble[5] with 750 particles. Parameters of the attempted moves were adjusted so as to reach the acceptance ratio about 30%. The cutoff parameters were set as follows: $R_c = 5\sigma$ for DLJD and $R_c = 12$ Å for water. In standard MD simulations with $N = 750$ particles we used the time step $\Delta t = 1$ fs and the SHAKE/Verlet method. Temperature was kept constant by the friction-like (Berendsen) thermostat[5] with the correlation time 2 ps.

In the case of systems with interface, an infinite lattice in the x and y directions is built up but there is no periodic extension in the z direction. The true 2D periodic sum is rather complex in this case. An efficient modification of the usual 3D Ewald summation has been derived by Yeh and Berkowitz[18]. The plain 3D sum is equivalent to an infinite periodic sum over slabs. The leading unwanted energy term originates from the slab di-

pole moment in the *z*-direction. If this term is subtracted, one gets effectively a single slab; note that the *z*-periodic symmetry is broken. The surrounding continuum is assumed to be metallic $\varepsilon' = \infty$. For the DLJD system, the cutoff was increased to $R_c^* = 6.4$.

In the GEMC simulations[27] the following ratio of the number of attempted moves per cycle (displacement and rotation):(volume change):(particle transfer) = $3N$:1:$20N$ was specified. We used 1150 particles in total. In the production runs the number of particles were fluctuating about 750 in the liquid phase and about 400 in the vapor phase with the volumes of the liquid and gas boxes being, approximately, the same. After an initial equilibration period we generated (in dependence on thermodynamic conditions) between 2–5 × 10^5 cycles to accumulate averages of the desired quantities.

The Ewald parameters for the DLJD fluid were set to $R_c = L/2$, $\alpha = 5/R_c$, and $K = 11$ in the case of bulk simulations. These parameters were chosen rather conservatively so that a trajectory, in comparison with a high-accuracy result, remained reproducible with high accuracy within 5,000 time steps and became essentially uncorrelated within 10,000 time steps. For the slab calculations, K was increased to $K_z = 20$ in the *z*-direction. For water, the Ewald parameters were set so as to guarantee an estimated error of the forces (in units of k_B K Å^{-1}) 0.05 in the *r*-space and 0.5 in the *k*-space[28]. Typical values are $\alpha = 0.3$ Å^{-1}, $K = 9$ for the box, and $\alpha = 0.19$ Å^{-1} and $K_z = 20$ for the slab.

To keep the development of the simulated systems under control, necessary control quantities were always monitored[29]. Statistical uncertainties (expressed as standard errors; precisely, estimated standard deviations of the averages) were obtained by a combination of the block (sub-average) method with determination of the autocorrelation coefficients[30]. The error estimates of the vapor density in the slab method include a slab asymmetry, i.e., the difference between the vapor densities on both sides of the slab.

RESULTS AND DISCUSSION

In order to facilitate comparison, we first run 'correct' simulations with the full Ewald summation and reaction field methods. They yield results in mutual agreement and are then used as a benchmark for a discussion of accuracy/appropriateness of the considered approximate methods.

Dipolar Fluid

The DLJD fluid was studied some time ago by Mecke et al.[20] To keep a contact with the results presented in their paper we consider therefore the same DLJD fluid at the same thermodynamic conditions. This means, the site–site span is set to $L^* = 0.515$ and homogeneous phases of the models with $\mu^* = 2$ and 3 are studied at $T^* = 2$ and 2.5, respectively.

Bulk Liquid

In Table I we summarize the benchmark results for the thermodynamic properties (internal energy and pressure) in the homogeneous phase. It is seen that both our new results (with reaction field and Ewald summation) mutually agree within small systematic errors explainable by different methodologies, and agree also with the older literature data. The results of approximate methods are collected in Table II. They all were obtained with the reduced cutoff $R_c^* = 5$, which is almost one half of the box size.

The pressure is calculated under the assumption that the virial of electrostatic force equals the electrostatic energy which is, as we will discuss in detail for water, less accurate than separate calculation of the virial of force of the SF-FG force.

We could not simulate the SF-FG potential by MD for $\alpha < 0.5$ because of implementation limitations caused by a combination of factors which separately do not pose problems: (i) an insufficiently smooth approximative SF-FG charge–charge interaction (discontinuous derivative of forces), (ii) approximation of function (*13*) by quadratic splines in which the initial discontinuity propagates during the construction of splines, and (iii) the ap-

TABLE I
The reduced internal energy U^*, pressure P^*, of the dipolar Lennard–Jones diatomic fluids at specified state points. Numbers in parentheses denote the estimated standard error of the last digits

μ^*	T^*	ρ^*	Reaction field		Ewald	
			P^*	U^*	P^*	U^*
2	2.0	0.53	n/a	–15.21083(54)	0.777(3)	–15.223(1)
3	2.5	0.5	n/a	–17.82492(83)	0.434(4)	–17.850(2)

proximation of a point dipole by two large charges close together so that the tiny spline error gets multiplied by a large number. This combination leads to heating of the system for $\alpha \leq 0.5$; the heating is negligible for $\alpha > 0.5$ because the jump is negligible (because of the fast decreasing erfc function in Eq. (*13*)). No heating occurs in the case of SP-M because the derivative of forces is continuous. (No heating occurs even if SP-M is approximated by splines, which is a bit slower than direct evaluation.)

TABLE II
Thermodynamic data of the dipolar Lennard–Jones diatomics obtained using different short-range electrostatic approximations

Approximation	Monte Carlo		Molecular dynamics	
	P^*_{VoF}	U^*	$P^*_{V=E}$	U^*
		State point: $\mu^* = 2$, $T^* = 2$		
Benchmark		–15.21083(54)	0.7768(29)	–15.2229(11)
SF-FG $\alpha = 0$	0.7992(38)	–15.12155(38)		
SF-FG $\alpha = 0.3$	0.7894(32)	–15.16307(75)		
SF-FG $\alpha = 0.5$	0.8036(35)	–15.04646(77)	0.8962(44)	–15.0389(11)[a]
SF-FG $\alpha = 1.0$	1.0518(44)	–14.0235(12)	1.3429(35)	–14.0250(12)
SP-M $c = 0.5$			0.7733(33)	–15.2263(11)
SP-M $c = 0.6$			0.7734(36)	–15.2237(14)
SP-M $c = 0.7$			0.7594(37)	–15.2386(11)
		State point: $\mu^* = 3$, $T^* = 2.5$		
Benchmark		–17.82492(83)	0.4345(34)	–17.8497(14)
SF-FG $\alpha = 0$	0.4793(23)	–17.60030(48)		
SF-FG $\alpha = 0.3$	0.4560(26)	–17.70619(49)		
SF-FG $\alpha = 0.5$	0.4729(31)	–17.43507(77)	0.7283(46)	–17.3931(21)[a]
SF-FG $\alpha = 1.0$	0.9378(28)	–14.84932(92)	1.7724(37)	–14.8530(18)
SP-M $c = 0.5$			0.4152(41)	–17.8394(23)
SP-M $c = 0.6$			0.4503(43)	–17.8511(21)
SP-M $c = 0.7$			0.4034(38)	–17.8781(23)

[a] $T^* = 2.006$ (first state point), $T^* = 2.528$ (second state point) in MD because of heating caused by the discontinuity in the derivative of the SF-FG forces.

Even if we omit the MD SF-FG results for $\alpha = 0.5$, we see that there is a small discrepancy between MC and MD results which is, according to our experience, caused by finite-size errors (the MD ensemble is not a true NVT ensemble), integration errors (finite time step) and thermostat errors (the last two reasons lead to a small violation of equipartition between the rotational and translational degrees of freedom). The SF-FG method works best with $\alpha = 0.3$. The SP-M method is best with $c = 0.6$ and even the assumption that the virial of approximated electrostatic forces equals the energy works well in this case.

Vapor–Liquid Equilibria

Table III summarizes the benchmark results on the vapor–liquid coexistence densities of the DLJD fluid. It is seen that the liquid densities obtained from the slab simulations are systematically lower by about 0.5% than the Gibbs MC results and the vapor densities are higher; in other words, the liquid is more volatile. This discrepancy is caused by the effect of truncation of the LJ potential (smoothly decreased to zero in interval $R_c \in [4.96,6.4]$). It is difficult to correct for this effect directly in the slab simulation as is the common practice in the bulk; in turn, the Gibbs MC results should be compared and the same holds for slab MD (all comparable simulations use the same LJ truncation).

TABLE III
Benchmark equilibrium vapor–liquid densities of the dipolar Lennard–Jones diatomic fluids obtained using different methods. Numbers in parentheses denote the standard error of the last digits

Method	ρ_l^*	ρ_g^*
	State point: $\mu^* = 2$, $T^* = 2$	
Gibbs ensemble	0.503892(44)	0.0056234(90)
Interface[a]	0.5039	0.0057
Interface	0.50145(9)	0.006715(20)
	State point: $\mu^* = 3$, $T^* = 2.5$	
Gibbs ensemble	0.481594(54)	0.007753(12)
Interface[a]	0.4809	0.0079
Interface	0.47763(8)	0.00843(2)

[a] Data taken from ref.[20]

Table IV provides results of approximate methods. With the exception of SF-FG with $\alpha = 1$, which is decaying very fast, the liquid densities are reproduced with an error of a few thousandths. Both Gibbs MC and slab MD give comparable results and only slab MD values are systematically shifted as explained above. These deviations are nevertheless well discernible within statistical uncertainties, which are by one order of magnitude smaller. The vapor densities are not so well reproduced and also statistical uncertainties are larger. We have also tried the same simulations with a shorter cutoff, $R_c^* = 5$. Not surprisingly, the results of approximate methods, not shown here, are worse.

TABLE IV
Equilibrium densities of the dipolar Lennard–Jones diatomic fluids obtained using different short-range electrostatic approximations

Approximation	Gibbs ensemble		MD + interface	
	ρ_l^*	ρ_g^*	ρ_l^*	ρ_g^*
	State point: $\mu^* = 2$, $T^* = 2$			
Benchmark	0.503892(44)	0.005623(9)	0.50145(9)	0.006715(20)
SF-FG $\alpha = 0$	0.503109(59)	0.005874(12)		
SF-FG $\alpha = 0.3$	0.50390(21)	0.005799(36)		
SF-FG $\alpha = 0.5$	0.50301(10)	0.006040(19)	0.50135(14)	0.006453(21)
SF-FG $\alpha = 1.0$	0.49334(14)	0.008900(33)	0.49107(12)	0.008686(32)
SP-M $c = 0.5$			0.50193(12)	0.005819(25)
SP-M $c = 0.6$			0.50218(13)	0.005577(17)
SP-M $c = 0.7$			0.50212(12)	0.006146(19)
	State point: $\mu^* = 3$, $T^* = 2.5$			
Benchmark	0.481594(54)	0.007753(12)	0.47763(8)	0.008431(18)
SF-FG $\alpha = 0$	0.48001(10)	0.008558(21)		
SF-FG $\alpha = 0.3$	0.48086(20)	0.008234(45)		
SF-FG $\alpha = 0.5$	0.47995(13)	0.009048(27)	0.47834(12)	0.009611(29)
SF-FG $\alpha = 1.0$	one phase		0.45200(13)	0.022471(58)
SP-M $c = 0.5$			0.47965(11)	0.008124(29)
SP-M $c = 0.6$			0.47915(11)	0.008010(24)
SP-M $c = 0.7$			0.47912(12)	0.008606(27)

Water

Most simulations for TIP4P/2005 water are carried out at ambient conditions, i.e., at T = 298.15 K and P = 1 bar which implies ρ = 997 kg m^{-3}. We also consider three additional elevated temperatures, T = 350, 450, and 600 K; the last one is supercritical for real water but subcritical for the used TIP4P/2005 water model.

Bulk Liquid

Similarly as for the DLJD fluid, the correct results for bulk water at ambient conditions are given in Table V. They include not only the internal energy, pressure, and coexistence densities, but also diffusivity, dielectric constant and the surface tension.

Results of various short-range approximations for bulk water are summarized in Table VI. Where both MC and MD are available, they are in a reasonable mutual agreement (MC gives systematically a slightly higher energy). As regards the quality of the short-range approximations, it is seen that SF-FG with α = 0.1 and 0.2 Å^{-1}, and SP-M with c = 0.6 and 0.7 give reasonably accurate results for both pressure and energy; SF-FG is better for pressure while SF-M for energy. (Although the deviations in pressure from the benchmark values look very large, one should bear in mind that the equivalent errors in density are small because the bulk modulus of water is 22 kbar; i.e., the error of 22 bar causes the density change of 0.1% only.) The above statement about pressure, however, holds true only if the pressure is calculated from the virial of approximated forces (P_{VoF}) or equiva-

TABLE V
The benchmark thermodynamic properties of the TIP4P/2005 model of water at ambient conditions (T = 298.15 K and ρ = 997 kg m^{-3}): residual internal energy U, pressure P, surface tension γ, diffusivity D, dielectric constant (relative permittivity) ε

Method	P, bar	U, kJ mol^{-1}	γ, mN m^{-1}	D, 10^{-9} m^2 s^{-1}	ε
Lit.	–18[a]	–47.69	69.8(10)[b]	2.08	60
Ewald	–1.1(35)[c]	–47.839(3)	68.9(7)[c]	2.10(2)	60.4(2.3)
RF	n.a.	–47.8178(83)			

[a] Ref.[19], recalculated. [b] Ref.[32], extrapolated. [c] Virial of force (VoF) values; P_{VVC} = –0.6(35) bar and γ_{VVC} = 68.3(7) mN m^{-1}.

lently from the virtual volume change (P_{VVC}). The assumption that the electrostatic energy equals the virial ($P_{V=E}$) gives worse results, especially for the SF-FG method while the SP-M method with c = 0.6 works well even in this case.

Out of many correlation functions describing the structure of water we choose three; the other correlation functions we have examined give qualitatively the same results.

1. The oxygen–oxygen radial distribution function (Fig. 3).

2. The first spherical harmonic expansion coefficient of the full oxygen–oxygen correlation function (Fig. 4; more accurately, we plot the difference $g_{100} - g_{010}$ taking into account the symmetry). This function describes the orientation of the molecular axis with respect to the vector connecting both molecules.

3. The cosine of the axis–axis angle (the dipole–dipole correlation function; Fig. 5).

The raw histogram data have been slightly smoothed to remove noise.

As regards the structure, the worst method considered is again SP-M with c = 0.8. On average, the SF-FG methods give better structure, sometimes with the exception in the first shell of particles (close to contact). The best structure results from SF-FG with strong damping ($\alpha \geq 0.2$ Å^{-1}); however, as

TABLE VI

The internal energy, pressure of the TIP4P/2005 water at T = 298.15 K, ρ = 997 kg m^{-3} obtained for 750 molecules using different simulation methods

Approximation	Monte Carlo		Molecular dynamics		
	P_{VoF}, bar	U, kJ mol^{-1}	$P_{V=E}$, bar	P_{VVC}, bar	U, kJ mol^{-1}
Benchmark		–47.8178(83)	–1.1(35)	–0.6	–47.839(3)
SF-FG α = 0	47(7)	–46.7115(42)	334.5(45)	50.7	–46.729(4)
SF-FG α = 0.1	25(9)	–47.2639(91)	173.1(46)	19.8	–47.275(4)
SF-FG α = 0.2	45(8)	–46.7955(92)	554.1(43)	21.0	–46.806(4)
SF-FG α = 0.3	93(9)	–44.1971(91)	2016.8(42)	101.7	–44.205(4)
SP-M c = 0.5			–85.4(46)	88.2	–48.010(5)
SP-M c = 0.6			16.2(48)	–49.0	–47.881(5)
SP-M c = 0.7			–231.9(47)	–29.1	–48.010(4)
SP-M c = 0.8			–893.8(47)	–153.6	–48.813(5)

we have already discussed, thermodynamic quantities are worse with this damping. Thus, $\alpha = 0.2$ Å^{-1} (dimensionless parameter $\alpha R_c = 1.2$) might be a practically useful compromise for SF-FG.

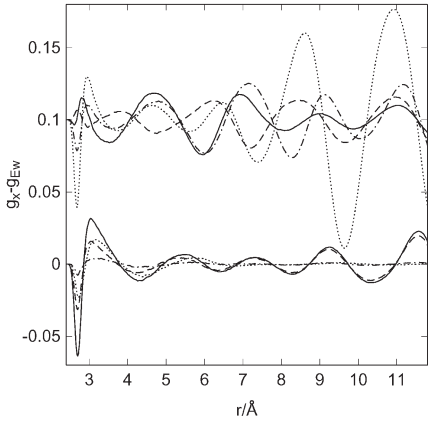

FIG. 3
Differences of the oxygen–oxygen radial distribution function from the Ewald method reference. Bottom curves: SF-FG; solid line: $\alpha = 0$, dashed line: $\alpha = 0.1$, dash-and-dotted line: $\alpha = 0.2$, dotted line: $\alpha = 0.3$. Top curves (shifted): SP-M; solid line: $c = 0.5$, dashed line: $c = 0.6$, dash-and-dotted line: $c = 0.7$, dotted line: $c = 0.8$

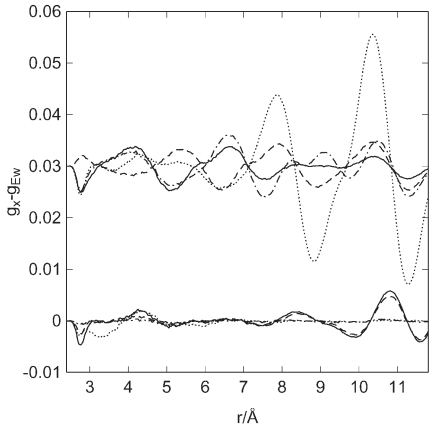

FIG. 4
Differences of the first harmonic coefficient from the Ewald method reference

Concerning possible artifacts, one should carefully examine the dipole–dipole correlation functions. They are systematically shifted to higher values. Although this shift is tiny, it cumulates if certain integrals are to be evaluated as, e.g., the Kirkwood factor leading to permittivity.

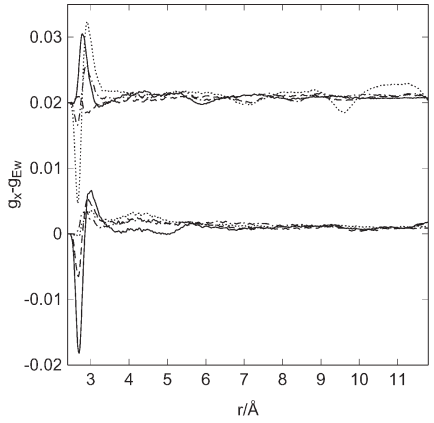

FIG. 5
Differences of the dipole–dipole correlation functions from the Ewald method reference

Vapor–Liquid Equilibrium, Surface Tension, Diffusivity and Dielectric Constant

'Benchmark' vapor–liquid coexistence densities for water obtained by different methods are collected in Table VII. First, it is seen that the MD results deviate systematically from the Gibbs-ensemble ones. This is caused by the truncation of the Lennard–Jones forces; we use a smooth truncation (similar as for charges) and R_c = 12 Å. At ambient conditions, the bulk correction is as high as –95 bar; with the compressibility about 5×10^{-5} bar^{-1}, this fully explains the observed deviation. Because of the condition of smooth forces in MD, it is difficult to include the corrections directly into the simulation in the slab geometry. It is therefore necessary to compare the MD and MC results separately.

The results of various approximate methods are given in Table VIII. We can see that the liquid densities calculated by short-range methods do not deviate, at moderate temperatures, by more than 1% from the precise values. Close to the critical point the differences evidently increase; the SF-FG method with α = 0.3 Å^{-1} does not predict a vapor–liquid equilibrium at all.

The best α (for SF-FG) or *c* (for SP-M) do depend on the conditions; the overall optimum setup is α = 0.1 Å^{-1} and *c* = 0.6. The SP-M variant works slightly better in this case.

Diffusivity, surface tension and dielectric constant at temperature 298.15 K are given in Table IX. Errors in diffusivity are a few per cent. The SF-FG works slightly better than SP-M. It is interesting to note that the error in the diffusivity calculated by different methods follows a trend similar to that of pressure: If pressure is underestimated (negative), the same holds for diffusivity. This can be viewed as another water 'anomaly'. For 'normal' fluids a higher pressure increases collisions of particles and slows down kinetics. On contrary, in water higher pressure leads to breaking of the hydrogen-bond network and enhances thus mobility. Anyway, the recommended methods (SF-FG with α = 0.1 Å^{-1} and SP-M with *c* = 0.6) give diffusivity barely distinguishable from the reference Ewald method result.

TABLE VII
'Benchmark' equilibrium vapor–liquid densities of the TIP4P/2005 model of water obtained using different simulation methods. Numbers in parentheses denote the error of the last digits

Method	ρ_l, kg m^{-3}	ρ_g, kg m^{-3}
	T = 350 K	
Gibbs ensemble	972.73(21)	0.08001(21)
Gibbs–Duhem[a]	971.3(12)	0.0823(2)
Interface	967.71(24)	0.09(1)
	T = 450 K	
Gibbs ensemble	883.81(21)	2.3032(54)
Gibbs–Duhem[a]	883.0(20)	2.34(1)
Interface[a]	879.0	2.42
Interface	879.13(19)	2.13(10)
	T = 600 K	
Gibbs ensemble	624.07(57)	53.25(16)
Gibbs–Duhem[a]	629.0(60)	59.3(13)
Interface	615.9(5)	56(3)

[a] Data taken from ref.[33]

TABLE VIII
Equilibrium vapor–liquid densities of the TIP4P/2005 model of water obtained using different short-range electrostatic approximations

Approximation	Gibbs ensemble (MC)		Interface (MD)	
	ρ_l, kg m^{-3}	ρ_g, kg m^{-3}	ρ_l, kg m^{-3}	ρ_g, kg m^{-3}
		State point: T = 350		
Benchmark	972.73(21)	0.08001(21)	967.71(24)	0.09(1)
SF-FG α = 0	967.81(22)	0.11171(32)	963.50(18)	0.11(1)
SF-FG α = 0.1	969.78(22)	0.09486(28)	965.96(20)	0.10(1)
SF-FG α = 0.2	970.78(24)	0.11417(37)	966.26(18)	0.09(1)
SF-FG α = 0.3	962.49(25)	0.25684(84)	960.25(14)	0.29(2)
SP-M c = 0.5			965.36(28)	0.06(1)
SP-M c = 0.6			969.13(20)	0.05(1)
SP-M c = 0.7			968.11(18)	0.12(4)
SP-M c = 0.8			973.18(25)	0.08(1)
		State point: T = 450		
Benchmark	883.81(21)	2.3032(54)	879.13(19)	2.13(10)
SF-FG α = 0	875.06(18)	2.9674(40)	872.13(17)	2.9(1)
SF-FG α = 0.1	879.87(24)	2.6663(75)	876.30(23)	2.8(1)
SF-FG α = 0.2	878.48(27)	3.1048(98)	876.48(18)	3.4(1)
SF-FG α = 0.3	857.42(32)	6.415(21)	855.42(21)	7.8(2)
SP-M c = 0.5			878.69(25)	2.5(2)
SP-M c = 0.6			880.96(17)	2.8(2)
SP-M c = 0.7			879.64(23)	2.1(3)
SP-M c = 0.8			887.63(24)	2.3(3)
		State point: T = 6000		
Benchmark	624.07(57)	53.25(16)	615.9(05)	56(3)
SF-FG α = 0	587.27(99)	78.18(45)	574.4(13)	72(3)
SF-FG α = 0.1	607.51(69)	67.72(29)	601.1(07)	65(5)
SF-FG α = 0.2	568.6(11)	90.60(50)	569.9(14)	75(1)
SF-FG α = 0.3	one phase		no interface	
SP-M c = 0.5			626.6(05)	57(4)
SP-M c = 0.6			625.3(04)	56(2)
SP-M c = 0.7			619.0(04)	54(2)
SP-M c = 0.8			647.4(02)	48(1)

The results for the surface tension include the Lennard–Jones cutoff corrections (of the first order). The first value, $\gamma_{V=E}$, has been obtained by assuming that the virial of force equals the electrostatic energy (which has been already proven to be less accurate). The second value, γ_{VVC}, has been obtained by a virtual surface change and corresponds to the standard virial of force; both values are the same within statistical errors as that obtained from the Ewald summation. It is seen again from the results of $\gamma_{V=E}$ that the virial theorem works poorly, especially for SF-FG, and should not be used. The values using the true pressure tensor are much more uniform with the exception of 'bad' parameters α = 0.3 Å^{-1} and c = 0.8. The SP-M version works slightly better.

The dielectric constant is the least precise quantity because it is calculated from fluctuations of total dipole moment. The short-range versions give on average slightly smaller values (which is not surprizing because part of the true electrostatic interactions is neglected) but the difference is not significant.

TABLE IX
Surface tension γ, diffusivity D, and dielectric constant ε, at 298.15 K obtained by molecular dynamics simulations

Approximation	$\gamma_{V=E}$, mN m^{-1}	γ_{VVC}, mN m^{-1}	D, 10^{-9} m^2 s^{-1}	ε
Ewald	68.9(07)	68.3	2.097(19)	60.4(23)
SF-FG α = 0	7.5(10)	66.4	2.167(25)	56.4(20)
SF-FG α = 0.1	34.0(10)	65.4	2.108(23)	60.0(22)
SF-FG α = 0.2	–44.5(10)	63.7	2.150(33)	54.6(19)
SF-FG α = 0.3	–335.0(10)	57.0	2.260(23)	60.0(26)
SP-M c = 0.5	102.0(10)	68.7	1.946(27)	56.8(22)
SP-M c = 0.6	54.7(13)	66.9	2.036(17)	58.8(23)
SP-M c = 0.7	105.7(12)	68.1	1.937(23)	56.4(24)
SP-M c = 0.8	208.8(15)	80.4	1.476(16)	63.9(32)

[a] Error estimates are the same as for $\gamma_{V=E}$.

CONCLUSIONS

For historical reasons (uncertainty of the correct treatment of the long-range forces) and applications of intermolecular potential models of water to complex systems, it would be common to use simple spherical cutoff even for models with strong long-range interactions. However, progress in computer hardware as well as development of new methods have made it possible to treat the long-range electrostatic interactions correctly and efficiently without the necessity of resorting to uncontrolled approximations such as the spherical cutoff[2,31].

Our analysis has shown that various short-range approximations of the Coulomb interaction can yield, if carefully implemented, also satisfactory results for many systems but no unique recommendation can be proposed. Questions that one should ask, and considerations that must be accounted for before a specific method is chosen, include:

1. What is the target accuracy?

If agreement with experimental data is the goal, the main source of error in most applications is the inaccuracy of the molecular model (the force field) which is not able (in principle or because a more accurate description is costly) to describe the rich world of interacting atoms. Then a faster though less accurate simulation method is legitimate.

In other applications, such as if the simulation results should serve as a basis for developing a statistical-thermodynamic theory or if a new force field is being developed, one should use as accurate method as possible. Using a short-range electrostatic would introduce an unacceptable dependence of the final theory or force field on the simulation method.

2. What are the quantities of interest?

Short-range electrostatic methods typically give well the structure (correlation functions) while thermodynamic quantities such as the internal energy and pressure are compromised. One should always check against the results of a correct method whether the system behavior is expected to rely on a balance between electrostatic forces, like for ions at interfaces, charged colloids, etc.

3. Careful optimization of parameters.

For the family of short-range methods, the cutoff R_c should be set to several molecular or atom diameters, at least about 5 for good results. An equally important property is the smoothness of the function approximating the true Coulomb energy and forces. (In fact, similar rules apply to the reaction field method.) Any function giving the true or slightly shifted forces at small separations and smoothly going to zero at the cutoff distance will

give good results. This is automatically satisfied for the SF-FG method. With the SP-M method, c close to unity gives a large 'bump' on the derivative of forces; consequently, the results are wrong[10].

To summarize, the product $R_c\alpha$ in the SF-FG method should range from 0 to 2, with the optimum perhaps around 1. Parameter c in the SP-M methods should be in the range 0.6–0.7. Parameters outside these ranges give poor results.

Parameters in the Ewald summation method should be generally set according to the charges in the system; estimates of errors are available[28]. As a rule of thumb, we recommend that $R_c\alpha > 3$ in the r-space sum, and $|k| < \alpha L$ in the k-space sum.

4. Potential model dependence.
The SF-FG method exhibits a jump in the derivative of forces. The jump may under some circumstances worsen the energy conservation in MD, especially for models with large charges close together and/or if a microcanonical ensemble is used. For usual models with moderate (partial or ionic) charges this effect is negligible and both SF-FG and SP-M methods are essentially equivalent.

5. Efficient calculation of forces.
Evaluation of the SP-M potential is faster than that of SF-FG because the erfc function is costly. Some efficiency can be gained by using splines but, according to our tests with SP-M, the direct evaluation of SP-M is still faster than the simplest quadratic splines.

6. Efficient calculation of pressure.
The equality of the virial of force and energy, which holds true for the exact electrostatic interaction, is violated for short-range potentials. This violation is especially bad for the SF-FG method and the pressure calculated in this way is very inaccurate. This drawback can be overcome by direct calculation of the virial of approximated forces; the computational cost is small for MD where the forces have to be calculated anyway, but larger for MC.

This research was supported by the Ministry of Education, Youth and Sports of the Czech Republic, Research Project No. 6046137307, and the Czech National Research Program "Information Society", Project No. 1ET400720409.

REFERENCES

1. Frenkel D., Smit B.: *Understanding Molecular Simulation*. Academic Press, San Diego 2002.
2. Sagui C., Darden T. A.: *J. Chem. Phys.* **2001**, *114*, 6578.
3. Smith W., Todorov I. T.: *Mol. Simul.* **2006**, *32*, 935.

4. http://www.vscht.cz/fch/software/macsimus.
5. Allen M. P., Tildesley D. J.: *Computer Simulation of Liquids*. Clarendon Press, Oxford 1987.
6. Barker J. A., Watts R. O.: *Mol. Phys.* **1973**, *26*, 789.
7. Neumann M.: *Mol. Phys.* **1983**, *50*, 841.
8. Steinbach P. J., Brooks B. R.: *J. Comput. Chem.* **1994**, *15*, 667.
9. Mahoney M. W., Jorgensen W. L.: *J. Chem. Phys.* **2000**, *112*, 8910.
10. Lísal M., Kolafa J., Nezbeda I.: *J. Chem. Phys.* **2002**, *117*, 8892.
11. Rick S. W.: *J. Chem. Phys.* **2004**, *120*, 6085.
12. Yonetani Y.: *Chem. Phys. Lett.* **2005**, *406*, 49.
13. Yonetani Y.: *J. Chem. Phys.* **2006**, *124*, 204501.
14. van der Spoel D., van Maaren P. J.: *J. Chem. Theory Comput.* **2006**, *2*, 1.
15. Mathias G., Egwolf B., Nonella M., Tavan P.: *J. Chem. Phys.* **2003**, *118*, 10847.
16. Solvason D., Kolafa J., Petersen H. G., Perram J. W.: *Comput. Phys. Commun.* **1995**, *87*, 307.
17. Fennell C. J., Gezelter J. D.: *J. Chem. Phys.* **2006**, *124*, 234104.
18. Yeh I.-C., Berkowitz M. L.: *J. Chem. Phys.* **1999**, *111*, 3155.
19. Abascal J. L. F., Vega C.: *J. Chem. Phys.* **2005**, *123*, 234505.
20. Mecke M., Fischer J., Winkelmann J.: *J. Chem. Phys.* **2001**, *114*, 5842.
21. Perram J. W., Smith E. R.: *J. Stat. Phys.* **1987**, *46*, 179.
22. Jedlovszky P., Pálinkás G.: *Mol. Phys.* **1995**, *84*, 217.
23. Steinhauser O.: *Mol. Phys.* **1982**, *45*, 335.
24. Eppenga R., Frenkel D.: *Mol. Phys.* **1984**, *52*, 1303.
25. Picálek J., Kolafa J.: *J. Mol. Liq.* **2007**, *134*, 29.
26. Zahn D., Schilling B., Kast S. M.: *J. Phys. Chem. B* **2002**, *106*, 10725.
27. Panagiotopoulos A. Z.: *Mol. Phys.* **1987**, *61*, 813.
28. Kolafa J., Perram J. W.: *Mol. Simul.* **1992**, *9*, 351.
29. Nezbeda I., Kolafa J.: *Mol. Simul.* **1995**, *14*, 153.
30. Flyvbjerg H., Petersen H. G.: *J. Chem. Phys.* **1989**, *91*, 461.
31. Sagui C., Darden T. A.: *Ann. Rev. Biophys. Biomol. Struct.* **1999**, *28*, 155.
32. Vega C., de Miguel E.: *J. Chem. Phys.* **2007**, *126*, 154707.
33. Vega C., Abascal J. L. F., Nezbeda I.: *J. Chem. Phys.* **2006**, *125*, 034503.